Supplementary Information for

Endotaxial Stabilization of 2D Charge Density Waves with Long-range Order

Suk Hyun Sung, Nishkarsh Agarwal, Ismail El Baggari, Yin Min Goh, Patrick Kezer, Noah Schnitzer, Yu Liu, Wenjian Lu, Yuping Sun, Lena F. Kourkoutis, John T. Heron, Kai Sun, and Robert Hovden

Supplementary Figure S1

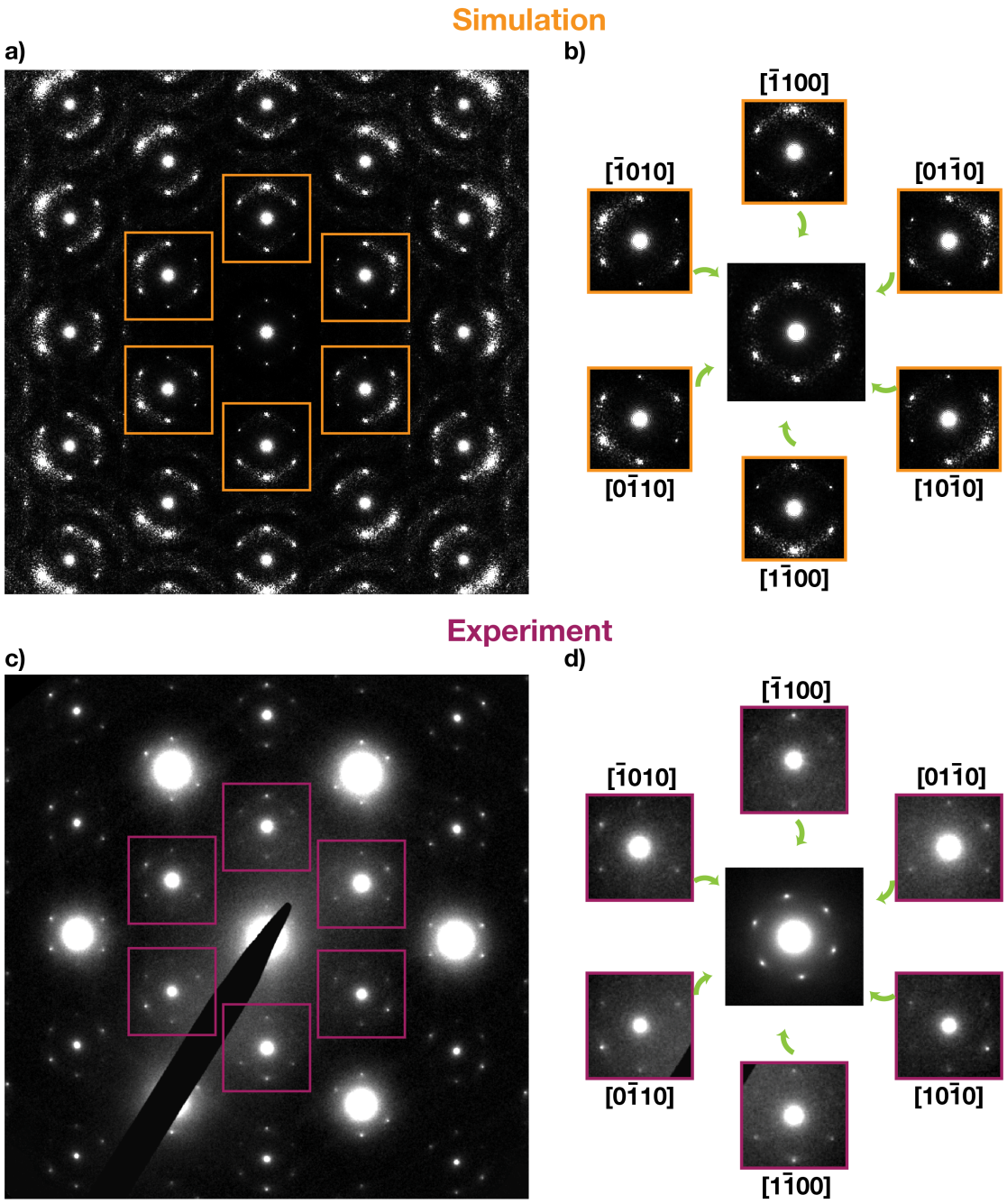

Fig. S1 | Removing CDW/PLD Diffraction Anisotropy. CDWs and PLDs manifest as satellite peaks in electron diffraction. Specifically, these superlattice peaks are anisotropically distributed around each Bragg peak [1–5]. This is clearly demonstrated in simulated (a) and experimental (c) diffraction pattern. b, d) For quantitative analysis, averaging six first order Bragg peaks evens out the anisotropy and enhances the signal to noise ratio.

Supplementary Figure S2

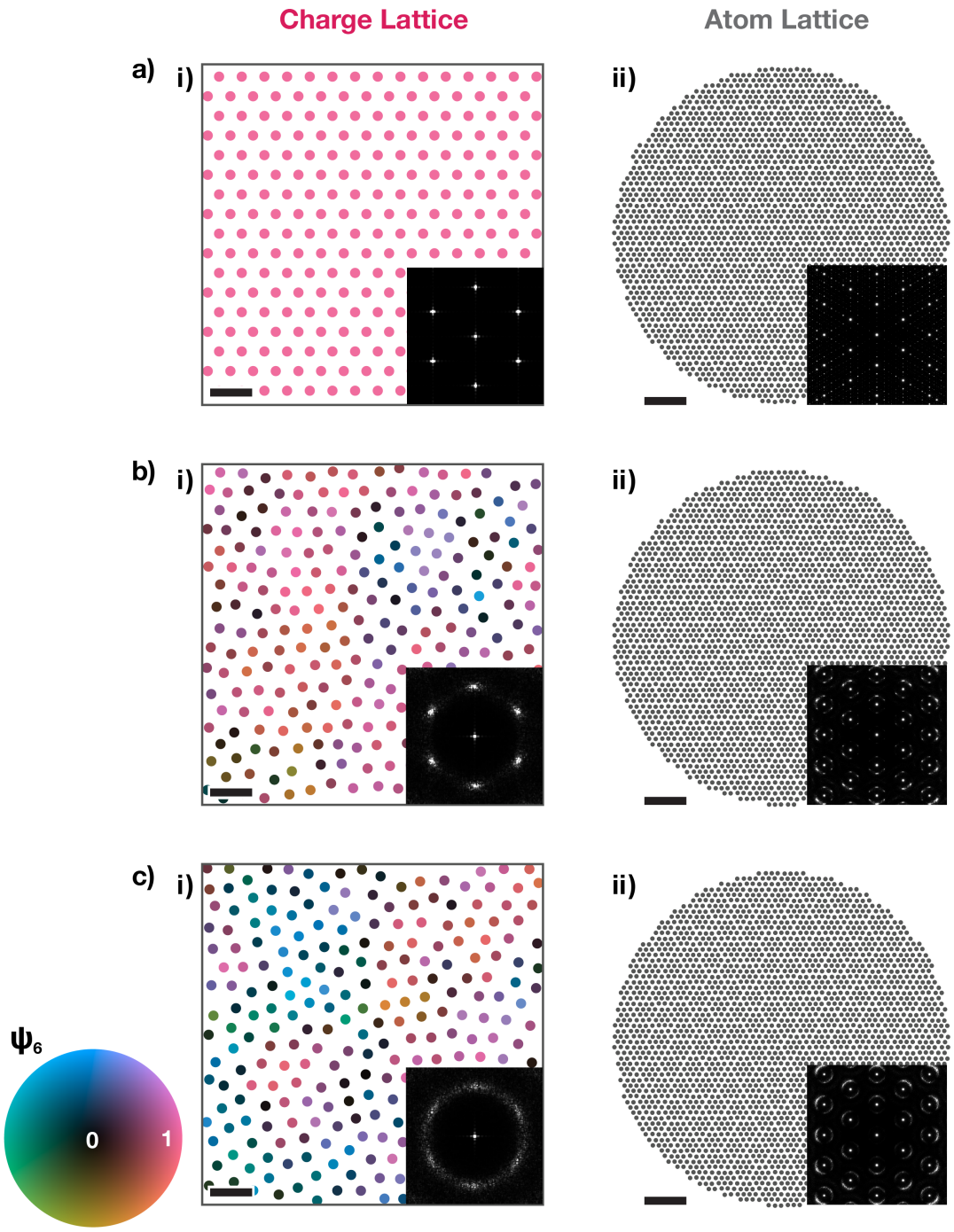

Fig. S2 | Simulated Hexatic Melting of Charge Lattice and Associated Atomic Lattice Distortion a-i) Pristine hexagonal charge lattice without disorder is presented. Structure factor (inset) shows sharp well defined six-fold symmetric peaks. a-ii) charge lattice attracts nearby atomic lattice sites forms clusters of atoms. Here, the charge and atomic lattices are incommensurate and each cluster is distinct. The clustering manifests as superlattice peaks decorating Bragg peaks. b-i) The charge lattice is thermally disordered—simulated by a Monte Carlo method (Metropolis-Hastings algorithm) using Boltzmann statistics and truncated Lennard-Jones potential for interparticle interactions. In 2D, crystal can melts hexatically and structure factor (inset) features characteristic azimuthally blurred peaks. c-i) Simulating with increased temperature further disrupts the charge lattice. Structure factor (inset) blurs azimuthally strongly. b, c–ii) Associated lattice distortion with disordered charge lattice is seemingly indistinguishable, however the structure factor (inset) shows azimuthally diffused superlattice peaks. Notably, the superlattice peak structure around each Bragg peak strongly resembles the structure factor of the charge lattice. Scale bars are 20 Å. Left-bottom) The magnitude and the argument of 6-fold bond order parameter ψ_6 is mapped to saturation and hue of the color wheel. The magnitude ($|\psi_6|$) and the argument ($\mathrm{Arg}[\psi_6]$) represents a amount of 6-fold orientational order and local orientation at each lattice site, respectively.

Supplementary Figure S3

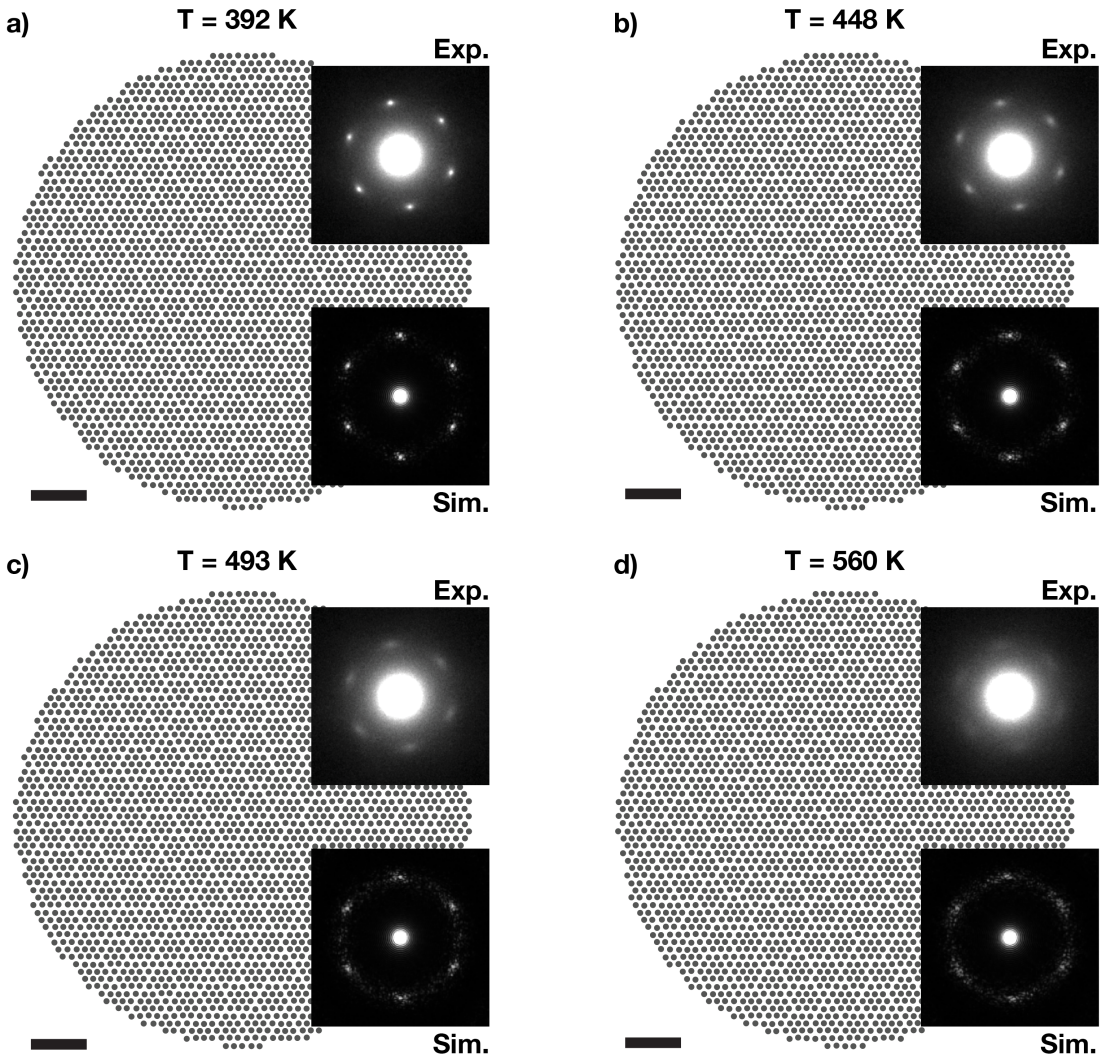

Fig. S3 | Comparison of Charge Lattice Model and Experimental Diffraction Patterns a–d) Increase in temperature (T = 392 K, 448 K, 493 K, and 560 K) disrupts CDW order, here simulated with hexatically melting charge lattice. Atomic lattice with associated lattice distortion displayed. The hexatic disorder azimuthally blurs the superlattice peaks. Simulated (inset-bottom) and experimental (inset-top) directionally averaged diffraction patterns qualitatively match. Scale bars are 20 Å.

Supplementary Figure S4

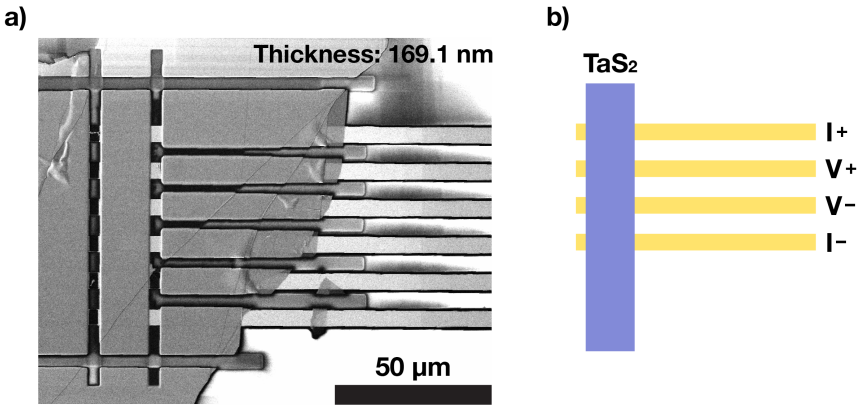

Fig. S4 | Electronic Device Overview. a) Scanning electron microscopy (SEM) image and b) schematic diagram of TaS_2 device. A flake of TaS_2 is transferred on to pre-patterned gold electrodes. The flake then was sculpted to a rectangular bar shape, using focused ion beam (FIB). The sample thickness was measured by atomic force microscopy (AFM).